

The growth of NaCl on flat and stepped silver surfaces

This article has been downloaded from IOPscience. Please scroll down to see the full text article.

2003 J. Phys.: Condens. Matter 15 6473

(<http://iopscience.iop.org/0953-8984/15/38/015>)

View [the table of contents for this issue](#), or go to the [journal homepage](#) for more

Download details:

IP Address: 171.66.16.125

The article was downloaded on 19/05/2010 at 15:14

Please note that [terms and conditions apply](#).

The growth of NaCl on flat and stepped silver surfaces

J Kramer, C Tegenkamp and H Pfnür

Institut für Festkörperphysik, Universität Hannover, Appelstraße 2, D-30167 Hannover, Germany

E-mail: pfnuer@fkp.uni-hannover.de

Received 2 May 2003

Published 12 September 2003

Online at stacks.iop.org/JPhysCM/15/6473

Abstract

The growth of thin NaCl layers at room temperature on a Ag(100) and a Ag(1, 1, 19) substrate has been investigated by LEED spot profile analysis, supplemented by EELS in order to clarify the electronic structure of the film. Our LEED analysis of NaCl/Ag(100) shows that the average orientation of the NaCl unit mesh is the same as that of the Ag substrate, but rotational mosaics are formed in the (100) plane. The angular distribution of rotational angles has a width of $\pm 9^\circ$ around the average direction. From this result we conclude that the direction of the substrate step edges determines the orientation of the NaCl islands. The steps of the vicinal silver surface are overgrown by elastic NaCl carpets. With increasing coverage, the modulation of the NaCl films by the step structure gets more and more washed out until, at around 10 ML, the whole film is only tilted by the nominal miscut of the sample. Closed films are only found at a thickness larger than 4 ML, as concluded from EELS.

1. Introduction

The growth of ultrathin epitaxial insulating films and possibilities to structure these films by self-organized processes is of high importance. Both on semiconductors and on metals such layers are needed to separate conducting material in ultra-small electronic devices of the future. In addition, epitaxial films allow detailed studies of local properties such as point defects in these films, which are of relevance both for electronic and for catalytic properties. This is why especially the properties of thin alkali halogenide films on semiconductors have been studied extensively in the recent past. A widely studied system in this context is NaCl/Ge(100). NaCl is a prototype wide bandgap insulator, the bulk properties of which are well known [1]. Thin NaCl films can be grown epitaxially on Ge(100) with high quality because of the small mismatch between the NaCl and Ge lattice constants [2–4].

Apart from the lattice mismatch the bond strength between the insulating film and the substrate, or, to be more precise, the site selectivity of adsorption, i.e. the corrugation of the potential energy surface at the interface, is also a further parameter controlling growth in this case. Therefore, investigations of the growth properties of NaCl on metallic substrates, which

have been carried out recently for Cu [5–7] and Al surfaces [8], are also instructive. Both on Cu and Al surfaces with various orientations epitaxial NaCl layers can be grown, but the crystallographic orientation of the close packed Al(100) and (111) substrates does not seem to have any influence on the orientation of NaCl islands [9]. In contrast, the growth of NaCl on Cu(111) forms well oriented islands, covering both terraces and steps [10]. On the Cu(100) surface NaCl is found to form narrow stripes and stripe arrays. The stripes are oriented parallel to the $\langle 110 \rangle$ directions [7].

The influence of steps can also be dramatic. On Cu the interaction of NaCl with steps is strong enough to restructure vicinal Cu surfaces [11, 12] with the result that a Cu(211) surface is transformed into a hill and valley structure consisting of (311) and (111) facets. The NaCl grows only on the (311) facets [11].

This motivated our study of the growth of NaCl on both on Ag(100) and on vicinal Ag(1, 1, 19). The use of LEED for studies of surface morphologies is not only a well established method, it also yields directly high quality average parameters of the surface not easily obtained by any scanning method. In contrast to tunnelling microscopy, LEED is not limited to ultrathin layers for insulating materials. The cubic lattice constant of silver differs by just 2.7% from the nearest neighbour distance of the NaCl crystal, which might favour epitaxial NaCl film growth with the unit mesh of the NaCl rotated by 45° with respect to the Ag substrate. This, however, was not found.

In order to quantify the role of steps in this system, we have also analysed the growth of NaCl layers on a Ag(1, 1, 19) surface. It consists of (001) terraces with close packed steps in the $[\bar{1}10]$ -direction. The nominal average terrace length is 9.5 atoms or 27.5 Å [13, 14] for steps of monatomic height. On the bare substrate this is indeed the strongly preferred step height [15], but with a rather broad distribution of terrace lengths around its mean value. This average terrace length is still large enough so that extremely thin NaCl films can still fully adjust to the registry on the single terraces. The role of the steps on thicker films will be important to answer the question whether insulating films on vicinal substrates can be pre-structured by the substrate morphology. This technique has been successfully applied to the NaCl/Ge(100) system both by using steps [16] and by modifying the Ge(100) surface with Na chains [17].

2. Experiment

The experiments have been performed in a UHV chamber operated at a base pressure of 1×10^{-8} Pa. It was equipped with a high resolution LEED and with photoelectron spectroscopy techniques. For EELS measurements, electrons with a primary energy of 50 eV have been focused onto the sample at an angle of 60° with respect to the surface normal, and the specularly reflected electrons with their characteristic losses have been measured. Thus we are sensitive primarily to dipolar losses. The backscattered electrons from EELS have been detected by a 150° spherical analyser ($r = 100$ mm).

The Ag(100) and Ag(1, 1, 19) samples used in this study have been mounted on a transferable sample holder. This holder also included a thermocouple (NiCr/Ni) connected to the sample holder near the sample surface, and a filament located behind the sample for radiative heating. All measurements have been performed at room temperature.

Surface cleaning in vacuum was achieved by sputtering and annealing cycles (Ar^+ sputtering at room temperature for 20 min at 2 keV, annealing up to 700 K). In order to achieve a clear spot splitting of the vicinal Ag surface in LEED, slow controlled cooling (2 K s^{-1}) of the sample to room temperature was necessary. Surface cleanliness was controlled by XPS. Thin NaCl films have been grown on the silver substrates at room temperature by evaporation of NaCl at an evaporation rate of $R = 0.3 \text{ ML min}^{-1}$. The thickness of the NaCl film was

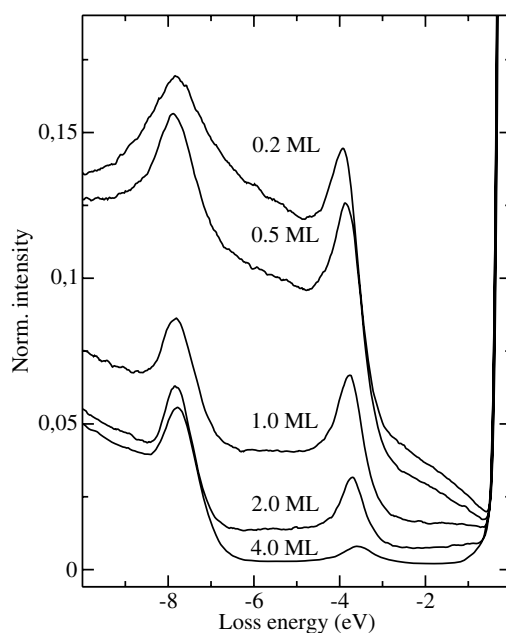


Figure 1. EEL spectra for various NaCl coverages. The spectra are measured at room temperature with a primary energy of 50 eV and they are normalized with respect to the elastic peak.

determined by using a quartz microbalance which was calibrated using the Na 1s and Cl 2p core-level intensities in XPS as a function of NaCl exposure.

3. Results and discussion

3.1. Morphological study of NaCl films on a Ag(100) surface

After preparation the quality of the films was controlled by EELS and XPS. As an example, EEL spectra as a function of the NaCl coverage are shown in figure 1.

The loss peak at 3.9 eV seen in all spectra is the well known interface plasmon with the expected shift to lower loss energy with increasing coverage. The excitonic excitation of NaCl at an energy of 7.8 eV [18] is seen already at the lowest coverages, but the bandgap of NaCl expected below the excitonic excitation is filled with a structureless background that increases with increasing loss energies. It is characteristic for the contribution of the Ag metallic surface. However, apart from this background no other characteristic losses have been found. The disappearance of any background in the bandgap indicates that the films are closed starting at a thickness of 4 ML. A similar island growth mode has been found for NaCl/Al(100) [8, 9] at similar growth conditions.

By increasing the electron dose considerably, it was possible to see loss structures in the energy range of 1.5–4.5 eV due to ESD induced colour centres and Na clusters [19]. Therefore, we conclude that stoichiometric and defect-free films (with a detection limit of 0.1% for surface colour centres) have been grown.

The morphology of the films at various thicknesses has been tested using spot profile analysis LEED. In figure 2 a LEED pattern for 1.6 ML NaCl, measured with an electron energy of 56 eV, is shown. The intense round spots are the integer order spots of the substrate. Additional strongly anisotropic spots from the NaCl film have the same symmetry and the same

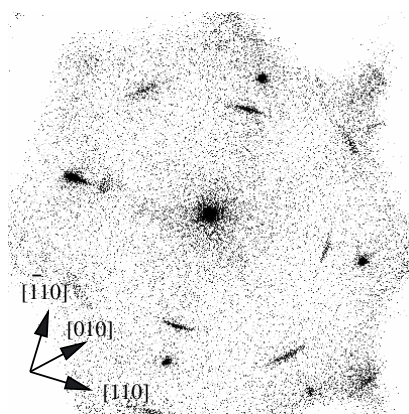


Figure 2. LEED pattern after evaporation of 1.6 ML NaCl onto the Ag(100) surface at room temperature, $E_{\text{prim}} = 56.0$ eV.

orientation as the substrate, i.e. the NaCl orientation is parallel to the main axes of Ag(100), not rotated by 45° . We found this arrangement of the NaCl film for coverages between a few per cent of a monolayer and 10 ML.

A lattice constant of 5.5 \AA for the NaCl film has been extracted from LEED patterns like that shown in figure 2, which have been taken at various electron energies using the Ag diffraction spots as reference. This lattice constant corresponds to a contraction by $\sim 2\%$ compared with the bulk lattice constant of NaCl of 5.63 \AA . No change of the lattice constant with increasing NaCl coverage up to a coverage of 4 ML could be observed.

Hebenstreit *et al* [9] also found a contraction of ultrathin NaCl films by 2–5% for NaCl/Al(111), although this system shows no specific orientation or registry of the NaCl film. This is in agreement with their calculations within the local density approximation, where the minimum energy was found at a lattice constant reduced by 5.7% for the monolayer and by 3.5% for three layers of a free NaCl film. From these results, and in agreement with our own measurements, it seems that the contraction of the lattice is characteristic for ultrathin NaCl films, but is not a result of a preferred registry with the substrate.

The azimuthal broadening of the NaCl induced LEED spots (see figure 2) is striking. The widths of the spots cover an angle of about 18° at all observable diffraction orders and independent of primary energy. This means that the orientation of the NaCl islands varies in a range of $\pm 9^\circ$ around the average orientation parallel to the unit mesh of the silver surface.

From the relatively small halfwidths of the NaCl spots in the polar direction, which increase very little with increasing diffraction order, we conclude that the NaCl film consists mainly of small crystallites that are well ordered internally. Mosaics are formed, which are rotated against each other, with the average $\langle 100 \rangle$ -direction of the NaCl film parallel to the $\langle 100 \rangle$ -direction of the substrate. Comparing the lattice constants of NaCl and Ag, a coincidence of every third NaCl unit mesh with every fourth Ag unit mesh is noted with a mismatch of 3.3%, i.e. the NaCl overlayer must be contracted by this amount with respect to the bulk lattice constant. Although the lattice contraction found here agrees closely with this value, there are several reasons why the coincidence between the Ag surface and the NaCl film is unlikely.

First, in the case of a coincidence lattice of NaCl, we expect to see additional spots in the LEED patterns, because the stress due to the mismatch must cause a local modulation of the nearest neighbour distances. We have examined the spot positions as a function of coverage and energy but could never see additional spots. On the other hand, the existence

of mosaics, which are rotated against each other by relatively large angles, and the almost uniform distribution of angles over the full range of variations cannot be understood, if the NaCl lattice preferentially locks in in a non-rotated direction. We therefore conclude that there is no detectable stress modulation of the films, and stress is not the major reason for the orientation and the orientational angular variation found.

It seems to be more likely that the (100) terminated NaCl islands start to grow at the substrate steps, where the van der Waals interaction is stronger than on the flat terraces, and, because of the step orientation, there is a clear directional force. In this case the angular spread of mosaic orientations must be caused by the angular variation of the step orientation of the original Ag surface. This variation on the bare Ag(1, 1, 19) surface was found to be around $\pm 12^\circ$ around the $\langle 110 \rangle$ direction, as deduced from the data of [15], which is not far from the $\pm 9^\circ$ of the NaCl mosaics, and therefore corroborates this interpretation. Nevertheless, preferential nucleation at step edges of the substrate is by no means trivial in the system discussed here, because the energetically favourable step directions (close packed rows in $\langle 110 \rangle$ -direction on Ag, non-polar steps in $\langle 100 \rangle$ -direction on NaCl) are not the same. Here several effects might help so that preferential growth is still in the $\langle 110 \rangle$ -direction. First, dipoles formed at interfaces, e.g. at nominally polar surfaces, are strongly shielded by the Ag metal, thus reducing their energy of formation, which in general is of the order of 1 eV/atom [16]. Second, diffusion of silver atoms at room temperature is large [14]: the orientation of the silver step edges fluctuates locally around the mean step direction. This allows easy local formation of kinks at the step edges and an efficient further reduction of the dipolar contributions of the NaCl on short length scales. Third, NaCl islands condensed at Ag step edges are likely to block the diffusion of Ag atoms and to freeze in the local step orientation so that relaxation may partly be incomplete. Thus, NaCl islands with slightly different orientations can be formed, in agreement with the observed spot broadening in LEED, and the main orientation of the NaCl islands is still determined by the average step orientation of the Ag(100) surface. It is clear that this mechanism only works if the diffusion of NaCl molecules on the Ag(100) surface at room temperature is high enough, so that all molecules reach a step edge during the mean diffusion path. As an alternative, the Ag surface could be forced to form $\langle 100 \rangle$ oriented steps. This, however, would easily lead to formation of multisteps on the vicinal Ag(1, 1, 19) surface, which was not observed.

These results differ to some extent from those obtained for NaCl growth on Cu(111) [6, 10] and Cu(100) [7] single-crystalline surfaces, where the interaction of NaCl seems to be stronger than with Ag so that elastic deformations play a more important role. Whereas on Cu(111) steps are decorated at room temperature, and NaCl forms nanometre sized crystallites and continuous films covering both terraces and steps of the Cu substrate, deposition of small amounts of NaCl on Cu(100) leads to the formation of narrow NaCl stripes oriented along the $\langle 110 \rangle$ directions [7]. For higher coverages, these stripes form a regular pattern with a fivefold superstructure. These phenomena are explained by strain relaxation at the edges of the strained adsorbate islands [7].

From the results on Cu(111) [6, 10] the authors suggest two growth modes. Whereas well oriented islands grow on the terraces, islands nucleated at step edges are supposed to grow with random orientation. Our LEED images cannot be explained with the existence of two kinds of NaCl islands. The NaCl induced intensity is concentrated in a small range of k -space, without any clear maximum. Therefore, the islands nucleated at the lower edges of substrate steps cannot be randomly oriented. On the other hand, the assumption of a low diffusion energy and the nucleation of NaCl films at step edges are corroborated.

On Al(111) and Al(100) surfaces, STM studies [8, 9] also done at 300 K reveal that $\langle 100 \rangle$ terminated NaCl(100) islands are formed, which are preferentially placed at the lower side of

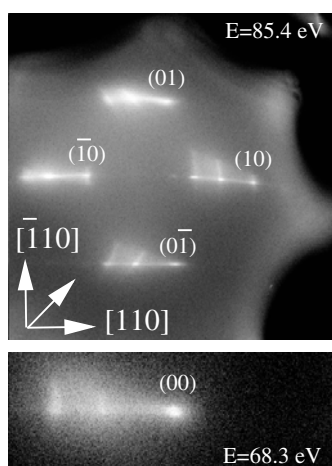


Figure 3. LEED pattern after evaporation of 5 ML NaCl onto the Ag(1, 1, 19) surface at room temperature: upper panel, first order spots of NaCl, $E_{\text{prim}} = 85.4$ eV; lower panel, (00) spot, $E_{\text{prim}} = 68.3$ eV.

the substrate step edges for both substrates. The orientation of the islands is not influenced by the crystallographic orientation of the substrate. The height of these NaCl islands is one layer. The formation of the second and third layers starts at a coverage of approximately 0.4 ML. These differences found for NaCl growth on close packed metal surfaces demonstrate that heteroepitaxy depends sensitively on subtleties of interactions and the energetic differences between various sites on these surfaces.

3.2. Morphological study of NaCl films on a vicinal Ag surface

In the following we examine the morphology of NaCl films grown on a vicinal silver surface, Ag(1, 1, 19) as a function of the coverage. In figure 3 we show a characteristic LEED pattern obtained after evaporation of approximately 5 ML NaCl at room temperature onto the Ag(1, 1, 19) surface at an energy of 85.4 eV (upper panel). Only the first order diffraction spots can be seen. The specular spot, not visible at this energy, is shown separately at an energy of 68.3 eV in the lower panel of figure 3. The spots of the silver substrate have disappeared and all integer order diffraction spots are broadened by a typical anisotropic halo on the side that points in the step down direction of the underlying substrate. These halos show two characteristic maxima in the intensity distribution. Similar halos can be found for coverages of 2.5 and 10 ML NaCl, but only one maximum is visible in the intensity distribution, respectively. The position of this maximum varies with layer thickness.

This behaviour is described more quantitatively by line scans along the $\langle 110 \rangle$ direction. In figure 4 examples are shown for the mentioned coverages. On the very right, the (00) spot, which decreases in intensity with increasing coverage, is visible. The origin of the satellites seen in figure 4 can be explained by plotting their positions in k -space as a function of k_{\perp} . Independent of the NaCl coverage, the observed maxima shift linearly to higher scattering vectors, k_{\parallel} , with increasing k_{\perp} over a wide range of incident energies. As an example, the positions of the two maxima of the 5 ML NaCl layer as a function of k_{\perp} are shown in figure 5. Linear fits through the data points intersect the (00) rod at its origin. This is a clear sign that these satellites are due to NaCl mosaics with characteristic angles of inclination with respect to

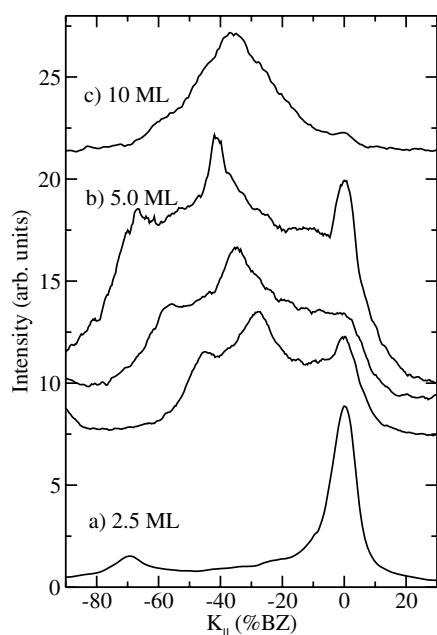


Figure 4. Spot profiles of the (00) beam in the [110]-direction for various NaCl coverages and scattering conditions. (a) 2.5 ML NaCl/Ag(1, 1, 19), $E_{\text{prim}} = 64.7$ eV; (b) 5.0 ML NaCl/Ag(1, 1, 19), from bottom to top $E_{\text{prim}} = 32.0$ eV, $E_{\text{prim}} = 53.1$ eV and $E_{\text{prim}} = 70.1$ eV; (c) 10 ML NaCl/Ag(1, 1, 19), $E_{\text{prim}} = 54.7$ eV.

the Ag(100) terraces, which are detected only on the vicinal Ag(1, 1, 19) surface with its high step density. The formation of facets or pyramids is not compatible with this behaviour. In this case, the data points should intersect the (00) rod at the closest three-dimensional Bragg point.

From the slope of the lines in figure 5 the angles of the mosaics were determined to be 3.2° and 5.2° with respect to the (100) orientation of the terraces of the silver substrate. It should be noticed that the first angle is smaller than the nominal miscut of the Ag(1, 1, 19) surface of 4.2° . This will be explained below. A similar behaviour was found for the 2.5 and 10 ML thick NaCl layers. The single satellite peaks found there correspond to mosaics with inclinations of 7.5° and 4.3° , respectively. The observed maximum mosaic angles obviously decrease with increasing coverage.

The reason for mosaic formation is most likely the misfit between the NaCl and the Ag lattice, particularly at steps. Steps of monatomic height of the NaCl lattice (2.82 \AA) do not fit to the steps of monatomic height of the Ag substrate (2.05 \AA), causing large electrostatic fields if they are forced to match. This problem, however, can be circumvented when the Ag steps are mostly overgrown by an NaCl layer that is elastically strained over many lattice constants forming an elastic carpet across the Ag steps. The NaCl film then consists of strained and slightly tilted sections close to the step edges and of flat parts, far away from the step edge. This is compatible with the findings that the carpet angles are getting smaller with increasing NaCl coverage and that the ratio of the halo intensity to the specular intensity increases with coverage. This means that the tilted parts of the NaCl films are getting flatter and more extended with increasing coverage. Carpet-like overgrowth of steps in order to avoid misfit dislocations is quite common for films out of ionic material and has been found for NaCl films both on semiconductor [2, 4] and on metallic substrates [9, 10].

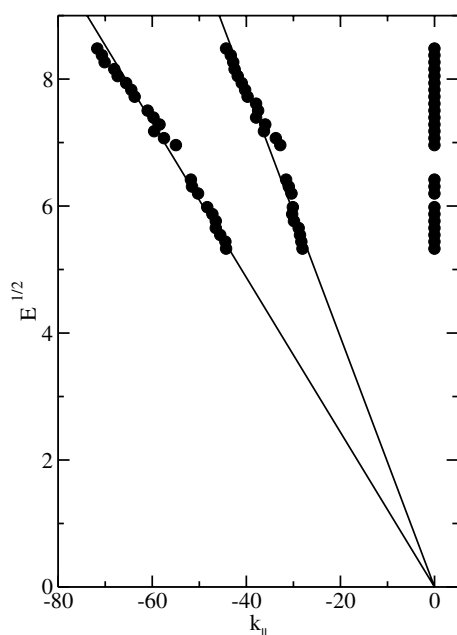


Figure 5. The position of the resolvable peaks seen along the [110]-direction for 5 ML NaCl/Ag(1, 1, 19). The solid lines show a linear fit to the data points.

In order to get more detailed insight into the properties and mosaic angles of the films in the case studied here, we use the model developed by Schwennicke *et al* [2], who neglected the discrete nature of the lattice and estimated the average length of the inclined zones close to a monatomic step within the scope of elasticity theory by minimizing the total energy of the adsorbed film. Bending the NaCl film, assumed to have a rectangular cross-section and a thickness d , across a step over a length Γ costs an increasing amount of energy if Γ is reduced, because of the increasing curvature of the film. This increase is compensated by allowing more molecules to be bound more strongly. Minimizing the sum of these two contributions yields [2]

$$\Gamma_{\text{opt}} = \left(\frac{3Ed^3a_0^2h^2}{16\epsilon_b} \right)^{1/4} \quad (1)$$

where E is the bulk modulus of the rod material, a_0 the NaCl lattice constant, h the height of a monatomic silver step and ϵ_b is the reduced binding energy of the NaCl film for the inclined areas. Equation (1) neglects additional lateral stretch of the NaCl films, because we expect that the films cannot be stretched laterally due to the missing influence of the crystallographic orientation of the substrate. This formula shows that the width of the inclined areas, Γ_{opt} , increases with increasing film thickness. The corresponding angle of inclination must therefore decrease for a constant step height. This model further assumes that the NaCl film is flat again at an appropriate distance from the step on both terraces adjacent to the step. With this information we can construct a model of the surface, which is shown in figure 6. The line scan for 2.5 ML thick NaCl film (see figure 4) shows only two peaks corresponding to the mosaics and to the flat terraces, respectively. At this thickness the above mentioned model seems to be fully valid. Steps are overgrown by carpets. From the mosaic angle of 7.5° the average length of the inclined zones, assumed to have a constant slope, can be determined to

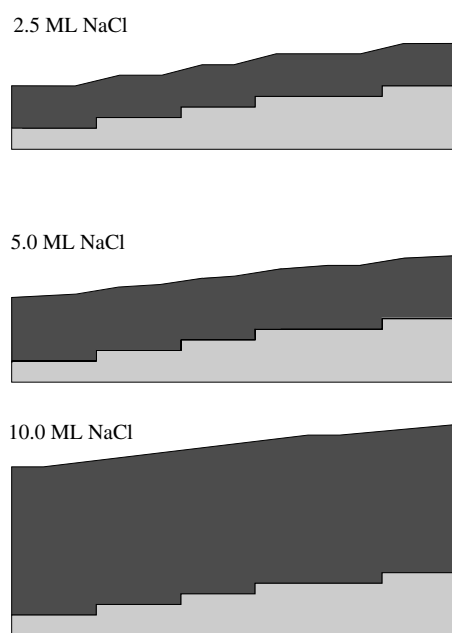


Figure 6. Schematic model of the NaCl surface for different coverages.

be $\Gamma_{\text{opt}} = 15.7 \text{ \AA}$. Deviations from this average length can be caused by the large variance of the terrace length distribution of the Ag(1, 1, 19) surface or due to a varying layer thickness on the surface. This results in broadening of the mosaic peak.

This average mosaic length is still small compared with the average terrace length. As a consequence, the reduced binding energy between the NaCl carpet and the Ag surface can be determined with equation (1). We obtain, within large limits of uncertainty, a value of $\epsilon_b = 0.21 \text{ eV}$. The binding energy of NaCl on a regular Ag(100) surface is not known. For NaCl/Ge(100) [2] $\epsilon_b = 0.13 \text{ eV}$ was obtained, which is one-tenth of the known binding energy of an NaCl molecule adsorbed on the Ge(100) surface. The value found here for NaCl/Ag(1, 1, 19) seems to be reasonable, since it is higher than on the semiconductor, but of the same order of magnitude.

In contrast, using equation (1), the expected length of distortion ($\Gamma_{\text{opt}} = 44.8 \text{ \AA}$) for high NaCl coverages (10 ML) is much larger than the average terrace length. This means that the NaCl film can no longer follow the full modulation by the steps of the silver substrate. The whole film is tilted around the nominal miscut of the substrate of 4.2° , and indeed, the position of the mosaic peak for the 10 ML film corresponds very closely to the average inclination of the substrate. The intensity distribution around the mosaic peak can again be explained by the length distribution of the silver terraces, which means that, for longer terraces than the average, partial relaxation is still possible. Therefore, full relaxation to the orientation of the substrate terraces has a small probability for this thickness of NaCl, which corresponds to the low LEED intensity in the specular direction.

Extending this analysis to the 5 ML NaCl film, $\Gamma_{\text{opt}} = 26.6 \text{ \AA}$ obtained from equation (1) is comparable with the average terrace width of the substrate. As a consequence, most parts of the film are expected to be tilted, and only partial relaxation can occur on the terraces so that the model used is no longer valid. Therefore, we can only give a qualitative interpretation, assuming that the growth mode is the same as for the other film thicknesses. There must still

be a characteristic mosaic angle, which for the 5 ML film should be in between the two others, which should correspond to the 5.2° inclination found for the mosaic peak with the larger inclination. Since the substrate terraces are too short to allow full relaxation to the orientation of the terraces, the NaCl films are expected to be modulated only, but all parts of the 5 ML film are inclined with respect to the substrate terraces. This explains the second mosaic peak with an angle of inclination of 3.2° found at this intermediate thickness, i.e. this peak corresponds to only partially relaxed parts on the terraces.

4. Summary and conclusion

From this study we conclude that the morphology of NaCl films grown on a Ag(100) substrate is strongly influenced by the step directions of the silver surface. Due to the high diffusion of Ag atoms at room temperature, the direction of the substrate steps shows little deviation from the $\langle 110 \rangle$ direction. As a consequence, single NaCl islands are also slightly rotated against each other and mosaics are formed on the surface. On average, the unit meshes of the NaCl and the silver substrate are oriented parallel. If we assume that the step edges of the silver surface are not influenced by the NaCl, we conclude, from the observed angles of rotation of the mosaics, that the silver steps deviate about $\pm 9^\circ$ from the $\langle 110 \rangle$ -directions at room temperature. From this model we expect a temperature dependence of the observed rotational angle, because the kink-formation frequency increases with temperature and the angle is getting larger. This prediction has not been verified yet because of experimental limitations.

Within this model, the observed mainly parallel orientation of the unit meshes remains to be fully understood, taking into account the large difference in step formation energies between polar and non-polar steps in ionic materials like NaCl. Considering only the step energy of NaCl, a step interface between Ag and NaCl with a rotation of the lattices by 45° seems to be more favourable, since it turns the NaCl step to a non-polar direction, but this orientation obviously does not minimize the interface energy between the two materials.

Within the models developed for the growth of NaCl on Ag(100), the results found on flat and vicinal surfaces do not contradict each other. They can be easily combined and reconciled, assuming that the growth mode switches, after nucleation at steps for the monolayer, to the carpet mode for thicker layers. Thus the films avoid the development of large Coulomb fields close to the step edges caused by the considerable lattice mismatch between Ag and NaCl. The latter mode has only been detected on the vicinal Ag(1, 1, 19) surface, because of the very low step density on the flat Ag(100) surface. At high step densities and for thick layers the carpet mode of growth leads to a uniform and only slightly modulated insulating film due to the high internal stiffness of the film. Thus the step orientation of the substrate determines the orientation of the insulator film, which is maintained after switching to the carpet mode.

Acknowledgment

We thank W Ernst and J Wollschläger for computational help and for useful discussions. This work was supported by the K&S AG, Kassel, Germany.

References

- [1] Roessler D and Walker W C 1968 *Phys. Rev.* **166** 599
- [2] Schwennicke C, Schimmelpfennig J and Pfnür H 1993 *Surf. Sci.* **293** 57
- [3] Lucas C A, Wong G C L, Dower C S, Lamelas F J and Fuoss P H 1993 *Surf. Sci.* **286** 46
- [4] Glöckler K, Sokolowski M, Soukopp A and Umbach E 1996 *Phys. Rev. B* **54** 7705

- [5] Fölsch S, Helms A, Zophel S, Repp J, Meyer G and Rieder K H 1999 *Phys. Rev. Lett.* **84** 123
- [6] Bennewitz R, Foster A S, Kantorovich L N, Bammerlin M, Loppacher C, Schär S, Guggisberg M and Meyer E 2000 *Phys. Rev. B* **62** 2074
- [7] Mauch I, Kaindl G and Bauer A 2002 *Surf. Sci.* **522** 27
- [8] Hebenstreit W, Schmid M, Redinger J, Podloucky R and Varga P 2000 *Phys. Rev. Lett.* **85** 5376
- [9] Hebenstreit W, Redinger J, Horozova Z, Schmid M, Podloucky R and Varga P 1999 *Surf. Sci.* **424** L321
- [10] Bennewitz R, Barwich V, Bammerlin M, Loppacher C, Guggisberg M, Baratoff A, Meyer E and Güntherodt H-J 1999 *Surf. Sci.* **438** 289
- [11] Fölsch S, Riemann A, Repp J, Meyer G and Rieder K-H 2002 *Phys. Rev. B* **66** 161409
- [12] Fölsch S, Helms A, Riemann A, Repp J, Meyer G and Rieder K-H 2002 *Surf. Sci.* **497** 113
- [13] Merikoski J and Ala-Nissila T 1995 *Phys. Rev. B* **52** R8715
- [14] Chang M F, Hoogeman M S, Klik M A J and Frenken J W M 1999 *Surf. Sci.* **432** 21
- [15] Kramer J, Tegenkamp C, Ernst W and Pfnür H 2003 *Surf. Sci.* **537** 265
- [16] Tegenkamp C, Ernst W, Eichmann M and Pfnür H 2000 *Surf. Sci.* **466** 41
- [17] Ernst W, Eichmann M, Pfnür H, Jonas K-L, von Oeyenhausen V and Meiwes-Broer K-H 2002 *Appl. Phys. Lett.* **80** 2595
- [18] Cox P A and Williams A A 1986 *Surf. Sci.* **175** L782
- [19] Zielasek V, Hildebrandt T and Henzler M 2000 *Phys. Rev. B* **62** 2912